Journal of Power Sources 205 (2012) 433–438

Contents lists available at SciVerse ScienceDirect

Journal of Power Sources

journal homepage: www.elsevier.com/locate/jpowsour

Silicon nanowire anode: Improved battery life with capacity-limited cycling

Vidhya Chakrapani, Florencia Rusli, Michael A. Filler, Paul A. Kohl*

School of Chemical and Biomolecular engineering, Georgia Institute of Technology, Atlanta, GA 30332, United States

ARTICLE INFO

Article history:
Received 25 November 2011
Received in revised form 5 January 2012
Accepted 5 January 2012
Available online 17 January 2012

Keywords:
Silicon nanowire
Ionic liquid electrolyte
Quaternary ammonium TFSI
Limited capacity discharge

ABSTRACT

Silicon nanowires grown on a stainless steel current collector were evaluated as Li ion battery anodes in an ionic liquid consisting of butyl-trimethyl ammonium bis(trifluoromethylsulfonyl)imide and lithium bis(trifluoromethanesulfonyl)imide. The electrodes showed good performance in the ionic liquid electrolyte with a stable discharge capacity of ~2000 mAh g^{-1} and coulombic efficiency of 97% after 50 cycles. However, the large internal stresses caused by the volumetric expansion of the Si during lithiation limits the long-term cycle life of the battery in both ionic and organic electrolytes due in-part to the repeated disruption and reformation of the solid electrolyte interface layer on the Si. In contrast, when the same Si nanowire electrode was cycled at relatively shallow discharges, similar to those of carbon anodes, 320 mAh g^{-1}, the battery showed better performance with cycle life greater than 650 cycles and coulombic efficiency close to 100% in the ionic liquid electrolyte. Cycling at 1000 mAh g^{-1} showed lifetimes in excess of 200 cycles in an organic electrolyte without cell degradation. The effect of Si doping, and amount of electrolyte in contact with the anode on the battery capacity and cycle life are also presented.

1. Introduction

There is currently interest in Si anodes for lithium ion batteries due to their high theoretical capacity. However, it is recognized that the high capacity of Si also leads to significant mechanical stain during lithiation that can cause cracking and deactivation of the electrode. Bulk or planar films cannot withstand high strain without catastrophic degradation of the electrode structure. Importantly, the use of Si-based anodes comprised of nanostructures such as nanoparticles, nanowires [1,2], and nanotubes [3], as well as novel morphological designs [4–6], can limit this damage and electrode performance up to few hundred cycles have been reported. However, a higher number of cycles, e.g. 1000 cycles, are desirable for secondary batteries, which have not been demonstrated.

Several strategies have been pursued to minimize capacity fade during cycling, such as mixing Si particles with conductive agents such as carbon [6–8], metal or metal silicide particles [9–11], carbon nanotubes [12], and graphene [13]. Encapsulation within a rigid outer shell such as Al_2O_3 [14], SiO_2 [15] or multi-walled carbon nanotubes [16], as well as the use of elastomeric binders [17], is also documented. Although these approaches do not alleviate the fundamental problem of volume expansion, they conserve electrical connectivity between the particles during structural degradation and considerable improvements in the cycle life have been achieved.

In situ stress measurement on Si thin films during lithiation and delithiation by Sethuraman et al. [18] showed that the film undergoes alternating compressive and tensile plastic deformation during lithiation and delithiation, respectively. At low state of charge, lithium incorporation into the Si induces a linear elastic change in mechanical strain. The films show a transition from elastic to plastic flow when silicon capacity reaches 325 mAh g^{-1}. Similarly, the films showed elastic to plastic behavior at higher depth of discharge, with maximum flow stress occurring at a discharge potential of 1.2 V. Thus, employing voltage cutoff limits during galvanostatic charging and discharging have helped in preventing the formation of a highly lithiated phase of Si, such as amorphous $Li_{4.4}Si$ that has the largest lattice constant among the various lithium–silicon alloys. Thus, it induces the maximum mechanical stress [19]. However, even with these strategies, battery life greater than a few hundred cycles without significant capacity fade is yet to be achieved.

Improvements in the battery life require optimization of the electrode structure as well as an appropriate choice of electrolyte. In a recent study, the combination of a quaternary ammonium based ionic liquid (IL) electrolyte and Si nanowire anode was reported [20]. IL electrolytes have several interesting features including a wide electrochemical potential window, high thermal stability (boiling point > 450 °C), and negligible vapor pressure. Half cell (Si/Li) and full cell ($Si/LiCoO_2$) measurements of nanowires in IL electrolyte showed steady discharge capacity of 2000 mAh g^{-1} even up to 50 cycles with columbic efficiencies over 97%. The extent of capacity fade was less than that measured for Si nanowires in commercially used $LiPF_6$ organic electrolyte.

* Corresponding author. Tel.: +1 404 894 2893; fax: +1 404 894 2866.
E-mail address: kohl@gatech.edu (P.A. Kohl).

0378-7753/$ – see front matter © 2012 Published by Elsevier B.V.
doi:10.1016/j.jpowsour.2012.01.061

In this paper, we address the two main failure mechanisms of Si-based anodes: large volumetric expansion during lithiation and poor electrical conductivity between particles after degradation. A limited-capacity cycling strategy (shallow depth of discharge) that enhances the lifetime of a Si nanowire anode in both IL and commercially used organic electrolyte is presented. In this approach, the battery was completely lithiated during galvanostatic charging; however, the depth of discharge was lower than full capacity during discharge in order to reduce the fraction of lithium extracted from the lattice and to minimize the disruption to the Si and its solid electrolyte interface (SEI) layer. This technique limits volume change during each cycle, therefore retarding mechanical degradation of the nanowires. Half cells of Si/Li, when cycled at a constant discharge capacities of 321 mAh g^{-1} (similar to a carbon anode) and 1000 mAh g^{-1} exhibited a tremendous improvement in the battery performance with cycle life (>650 cycles and columbic efficiencies close to 100%). Finally, in order to improve the electrical conductivity, doped nanowires were synthesized and their effect on the battery capacity and cycle life were measured.

2. Experiments

Doped and undoped Si nanowires were grown via chemical vapor deposition with an Au catalyst on stainless steel current collectors (type 304, McMaster Carr). Stainless steel substrates were initially cleaned using a standard UHV cleaning procedure, which is described elsewhere [20]. A 5 nm Au catalyst layer was subsequently deposited by e-beam evaporation at 10^{-7} torr. Si nanowires were grown at 550 °C using SiH_4 in a H_2 carrier gas at a total pressure of 15 Torr for 20 min. The SiH_4 partial pressure during all growth runs was maintained at 1.4 Torr. Doped nanowires were grown at the same conditions as undoped nanowires except for the co-flow of a dopant-containing precursor gas. Phosphine (PH_3) was used as the precursor for n-doping with the P:Si gas phase ratio set at 0.002:1. Trimethylboron ($B(CH_3)_3$) was used for p-type doping with a B:Si gas phase ratio of 0.002:1. It is important to note that the stainless steel substrate reacted with both the dopant gases and significant conformal deposition of Si was observed. To mitigate this, a 50 nm doped amorphous Si (a:Si) was deposited on stainless steel substrate by plasma enhanced chemical vapor deposition (PECVD) prior to Au evaporation and nanowire growth. This film was deposited using 500 sccm SiH_4 at a total pressure of 1000 mTorr and a substrate temperature of 200 °C for 15 min. The flow rate of the phosphine (n-dopant) or diborane (p-dopant) precursor gases was maintained at 50 sccm. The RF power during deposition was 50 W. After deposition of the a:Si, the 5 nm Au catalyst was evaporated for Si nanowire growth.

Using the same nanowire growth conditions as described above, improved nanowire yield was obtained (1.6 mg cm^{-2}) in the presence of a:Si layer compared to the 0.63 mg cm^{-2} weight of nanowires grown without the a:Si intermediate layer. The a:Si layer probably served as a secondary Si source during the nanowire growth which resulted in a highly dense nanowire mat. The average dopant concentration in the nanowires, was measured by secondary ion mass spectroscopy (SIMS) for both boron and phosphorous. Quantitative determination of the dopant concentration in the nanowires using SIMS is problematic because of the shape of the nanowire (i.e. non-planar) and inability to obtain reliable depth profiles. Hence, the values reported here are semi-quantitative and are used to confirm the presence dopants in the wires. To minimize exposure to air and limit oxide formation, the Si nanowires were transferred to an Ar filled glove box immediately following growth.

The as-grown nanowires were used as the anode for electrochemical testing without the addition of a conductive agent or binder. Before testing the electrode, its mass was determined using a Metler microbalance. Electrochemical tests were performed in a split flat cell (MTI Corp.) using a metallic lithium foil as counter and reference electrode and Celgard as the separator. 1 M $LiPF_6$ in 1:1 mixture of ethylene carbonate (EC) and dimethyl carbonate (DMC) served as the organic electrolyte. The IL electrolyte was composed of 1.0 M of lithium (trifluoromethanesulfonyl) imide (LiTFSI) in butyl trimethyl ammonium (trifluoromethanesulfonyl) imide (QA-TFSI). 10 wt.% propylene carbonate (PC) added to this mixture to promote the formation of an SEI layer. All chemicals were purchased from Sigma–Aldrich. Galvanostatic cycling of the cells was performed using an Arbin, Inc., battery tester. All electrochemical measurements were completed in an Ar filled glove box, whose H_2O concentration was maintained below 0.1 ppm.

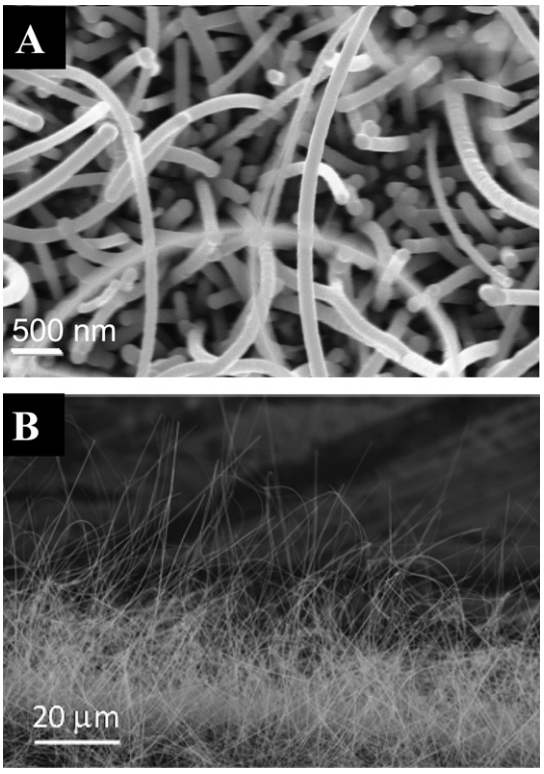

Fig. 1. SEM images of Si nanowires grown on stainless steel substrates. (A) Top down image showing randomly oriented nanowires with diameters in range of 80–100 nm. (B) Cross sectional image showing nanowires, which are several 100 μm in length.

Scanning electron micrographs (SEM) were recorded using a Zeiss Ultra60 field emission microscope. In order to observe the morphology and microstructure of the electrode after electrochemical testing, nanowire electrodes were soaked overnight in neat DMC to remove excess salt and high boiling solvent. Compositional analysis of the electrolyte was done by thermal gravimetric analysis (TGA), which was recorded using TGA-Q50 (TA Instruments-Waters LLC).

3. Results and discussion

As-prepared electrodes consisted of a mat of random oriented Si nanowires, with diameters ranging from 80 to 100 nm and lengths in excess of several hundred micrometers, on a stainless steel substrate. The doped and undoped nanowires were high crystalline as evidenced by the high resolution SEM images (Fig. 1A) and XRD spectra (not shown), which are consistent with previous reports on nanowires grown under similar conditions. Fig. 1A and B shows SEM images of a typical electrode. No significant differences in

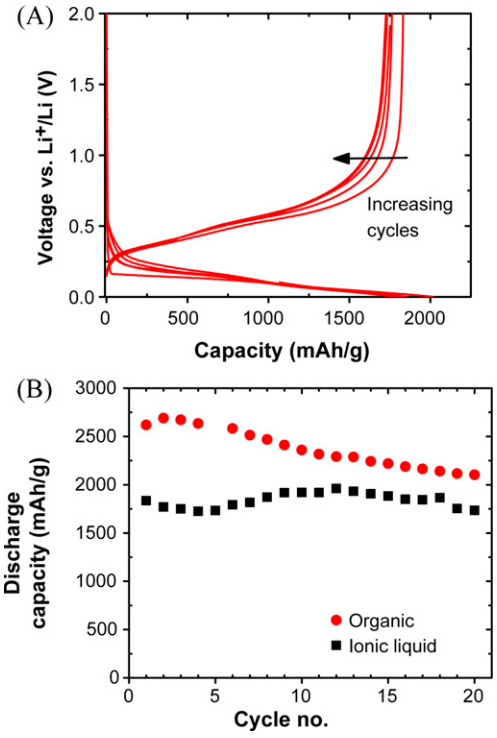

Fig. 2. Comparison of the cycling performance of Si nanowire anode in 1 M $LiPF_6$ in 1:1 EC/DMC organic electrolyte and 1 M LiTFSI/QATFSI IL electrolyte containing 10 wt.% PC. The electrodes were cycles at a C/20 rate between 0.001 and 2.0 V vs. Li^+/Li.

the morphology were observed between the doped and undoped nanowires.

Fig. 2A shows the galvanostatic cycling of nominally undoped Si nanowires in IL electrolyte, consisting of 1 M LiTFSI in QATFSI and 10 wt.% propylene carbonate (PC) at a C/20 rate. PC was added to decrease the viscosity and ionic resistivity of the electrolyte and promote the formation of a stable SEI layer on silicon [20]. The electrodes showed good chemical and electrochemical stability, with first cycle charge and discharge capacities of 2014 mAh g^{-1} and 1836 mAh g^{-1}, respectively. The columbic efficiency was 91% for the first cycle indicating modest consumption of PC to form the SEI and other parasitic reactions, such as co-intercalation of $TFSI^-$. The high capacity obtained for nanowires is partly due to the porous structure of the electrode, which allows for the volumetric expansion during lithiation. Preliminary measurements in organic electrolyte indicate that the battery capacity depends strongly on the packing density of the electrode. To obtain electrodes with different porosity, the growth time for the nanowire samples was 10, 20, 40 and 60 min. The maximum capacity was obtained for nanowires grown for 20 min. Capacity loss was seen for highly dense nanowire mats, which may be partly due to the lack of accessability of the wires to the electrolyte. All measurements reported here were done with nanowires grown for 20 min. The silicon nanowire half-cells were tested for long term cycling stability at a C/20 rate and the results are summarized in Fig. 2B. Also shown are the results of the nanowires tested in LiF_6 organic electrolyte. The IL electrolyte yielded first cycle charge and discharge capacities of 3029 and 2641 mAh g^{-1}, respectively. The change in the capacity of the nanowires in the IL electrolyte during the first 15 cycles is associated with the formation of the SEI layer on the silicon surface. The subsequent decay in capacity is associated with irreversible losses such as mechanical degradation of the electrode and reformation of the SEI. The capacity retention of the nanowires after

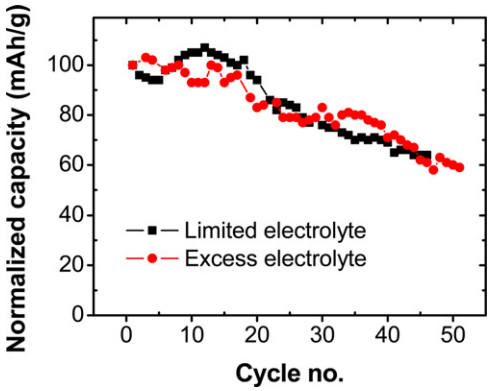

Fig. 3. Effect of limited (0.5 ml) versus excess IL electrolyte (10 ml) on the cycling performance of Si nanowire anode. The composition of the electrolyte in both cases was 1 M LiTFSI–QATFSI with 10 wt.% PC. Shown here is the discharge capacity normalized to the value observed for the first cycle.

20 cycles in IL electrolyte was 94.5%. In comparison, the capacity retention of nanowires was 80% when cycled in $LiPF_6$ organic electrolyte.

Although the nanowire electrode showed good performance up to 50 cycles in both IL and organic electrolyte, long-term capacity fade still limits battery performance. The large volumetric change of the Si nanowires during cycling generates internal stresses that mechanically degrade the Si nanowire, and is ultimately responsible for loss of electrical connectivity with the current collector. XRD spectra and high resolution SEM images of the electrode taken after electrochemical cycling showed that nanowires were mostly amorphous, as shown in Fig. S6 in Supplementary Information. This is consistent with the results of Chan et al. [21] who showed that the nanowires undergo irreversible crystalline-to-amorphous transition during lithiation. In addition, the continuous expansion/contraction of the wire results in cracks and the loss of structural integrity of the SEI layer. In addition to affecting the battery performance, it also results in continuous consumption of electrolyte due to the reformation or repair of the SEI layer during each cycle. In such cases, the battery life is limited by the availability of the electrolyte or SEI forming additive. This is an especially important concern for batteries employing ionic liquid electrolyte where external additives, such as PC, are added in small quantities (typically 2–10 wt.%) to promote the formation of the SEI layer.

To probe the cause of capacity fade seen with IL electrolyte, the performance of the Si nanowire electrode was measured in both limited (0.5 ml of electrolyte) and 20 times excess (10 ml of electrolyte) ILs containing 10 wt.% PC. The superficial electrode areas in both runs were approximately 3.2 cm^2. The separation distance between the two electrodes was kept nearly constant to avoid changes in the electrolyte resistivity. Fig. 3 shows the normalized discharge capacity for a Si nanowire electrode measured for both of these cases and reveals little difference in capacity fade up to 50 cycles. Thus, we conclude that the observed capacity fade is likely unrelated to the availability of PC, but rather due to mechanical disintegration of the Si nanowires.

Although the mechanical strain during lithiation and delithiation cannot be avoided, they can be retarded to a significant extent by limiting the amount of lithium inserted into the lattice or removed during discharge. In situ stress measurements studies by Sethuraman et al. [18] on Si thin-films during lithiation and delithiation show that at low state of charge, the compressive mechanical stress is mainly elastic with strain, and increases with an increase in lithium loading. However, the films showed a transition from elastic to plastic regime when the Si capacity reached 325 mAh g^{-1}.

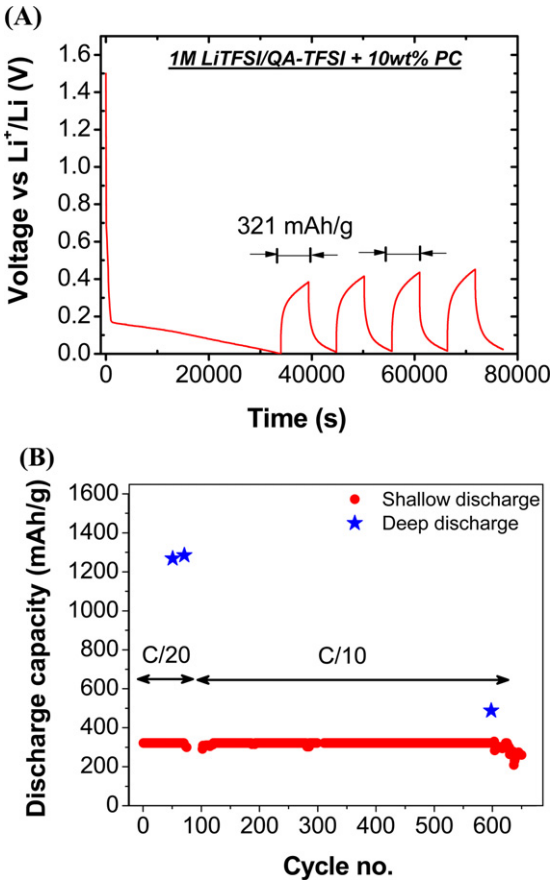

Fig. 4. Performance of Si nanowire anode in 1 M LiTFSI/QATFSI electrolyte containing 10 wt.% PC during limited capacity discharge of 321 mAh g^{-1} cycling. (A). Voltage vs. time profile of the cell during cycling. The cell was charged to a potential of 1 mV vs. Li^+/Li after each discharge cycle. (B). Cycle life of the battery discharged initially at C/20 rate and then subsequently at C/10 rate. Data points indicated by star (★) represent battery capacity during full discharge.

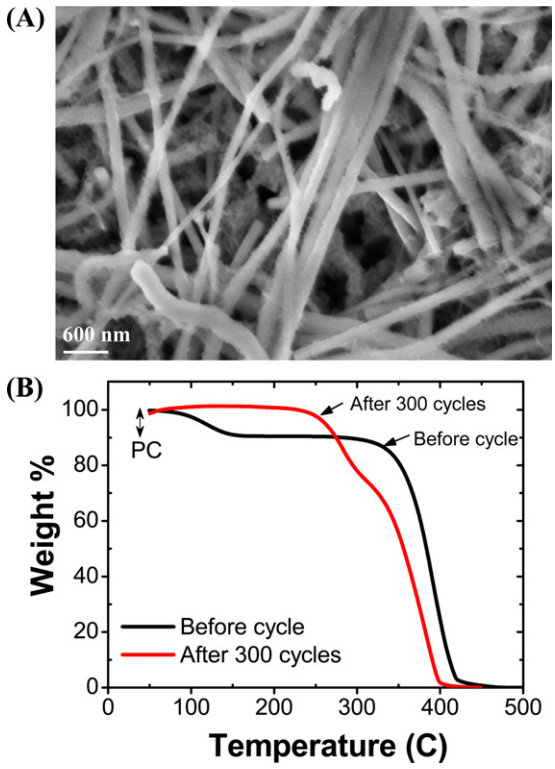

Fig. 5. (A) Scanning electron micrograph of Si nanowire anode after 650 discharge cycles. (B) Thermo gravimetric analysis of the IL electrolyte before and after 300 charge/discharge cycles. The plateau seen at ~120 C for pristine electrolyte, and which is notably absent in the spectra taken with electrolyte after battery cycling, indicate complete loss of PC after 300 discharge cycles.

The films showed a similar behavior, but in opposite direction, during discharge with elastic to plastic transition occurring at higher depth of discharge. They showed that the maximum tensile stress occurs at a discharge potential of 1.2 V and the film undergoes alternative compressive and tensile plastic deformation during cycling. These data indicate that battery life can be improved by cycling the electrode within a limited capacity regime. There are several advantages to this approach. By cycling between a constant state of charge and depth of discharge, nanowires undergo a constant volumetric variation during each cycle. Further, reducing the total amount of discharge reduces the fraction of lithium inserted into the lattice and the extent of lattice strain. Secondly, avoiding wide swings in the potential preserves the SEI layer, which is destroyed during discharge, and reduces unwanted electrolyte consumption for the SEI formation during each cycle. While it may seem counter-productive to use a high capacity Si anode and then limit its capacity, the capacity of a shallow discharged Si anode can be as high or higher than a traditional carbon anode with other potential benefits, such as high surface area (high power) or longer cycle life.

To this end, Si nanowire electrodes were cycled at limited discharge capacity in both IL and organic electrolytes. Fig. 4A shows the typical voltage vs. time profile of a nanowire anode in the IL electrolyte during shallow discharges. The battery was charged to a voltage of 1 mV vs. Li^+/Li for all cycles. Discharge cycles were limited to a capacity of 321 mAh g^{-1} of Si mass. The value of 321 mAh g^{-1} was selected to enable a comparison of cycling performance for Si anodes and commercially used carbon anodes with the same rated capacity.

Fig. 4B shows the cycle life of the battery during shallow discharges. The cell containing an IL electrolyte was initially charged and discharged at a C/20 rate until 80 cycles, after which it was cycled at the higher rate of C/10, and yielded a cycle life greater than 650 cycles. Compared to full cell discharge experiment shown in Fig. 2B, it is clear that the battery life can be greatly improved with this shallow capacity cycling approach. The coulombic efficiency of the cell during shallow discharging was 99.2%, which indicates little capacity loss through SEI formation. To determine the full rated capacity, the battery was occasionally allowed to undergo a complete discharge to 2.0 V vs. Li^+/Li. The value of the full capacity is also shown in Fig. 4B. After 600 cycles, the battery exhibited a capacity of 550 mAh g^{-1} on full discharge. However, this value is probably not representative a battery cycled at 321 mAh g^{-1} without undergoing deep discharges to measure the capacity due to the degradation that occurs upon deep discharge. It is important to note that the capacity of a battery undergoing only shallow discharges (i.e. 321 mAh g^{-1}) would most likely be higher than the one reported here. The silicon nanowire anode in the ionic liquid electrolyte showed a cycle life greater than 650 cycles at C/10 capacity. It should be noted that the cycle life reported here is higher than that reported for a carbon anode in an IL electrolytes, so far.

Changes in the morphology of the Si nanowire electrode after electrochemical testing, was analyzed using SEM. The SEM image shown in Fig. 5A reveals that nanowires retain their morphology after 650 limited capacity charge–discharge cycles. Thermal gravimetric analysis of the IL electrolyte was completed intermittently during battery cycling to examine changes to electrolyte composition. Fig. 5B shows the changes in the weight of the electrolyte

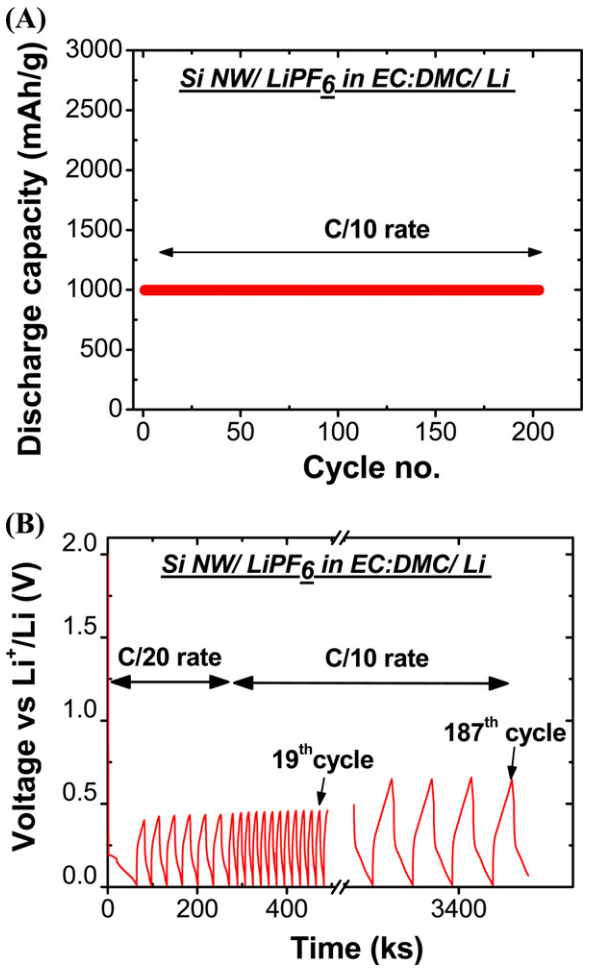

Fig. 6. (A) Voltage–time profile of the n-doped Si nanowire anode in 1 M LiPF6/EC/DMC organic electrolyte when discharged at 1000 mAh g^{-1} capacity. (B) Cycle life of the battery during limited-capacity discharge at C/10 rate in organic electrolyte.

during an isothermal ramp. The electrolyte was tested before and after undergoing 300 shallow charge–discharge cycles. The TGA curve for the electrolyte before any electrochemical testing shows two plateaus. A gradual loss of weight starts at ~90 °C and reaches a maximum of 10% change at ~170 °C due to the evaporation of the organic additive, propylene carbonate. Complete weight loss for the ionic liquid (LiTFSI/QATFSI) was seen at ~400 °C. A comparison of TGA results for IL electrolytes both before and after electrochemical testing reveals that most of the PC is consumed within the first 300 cycles. Interestingly, the absence of PC, which is the SEI forming additive, does not immediately degrade the battery performance because the cell underwent an additional 350 cycles. This is consistent with our hypothesis that the SEI layer is mostly preserved during the shallow charge/discharge cycling and hence doesn't require the presence of significant amounts of PC. The loss of PC seen during the first 300 cycles probably occurred during the deep charge–discharge cycles.

Additional limited depth of discharge measurements were made at a higher discharge capacity corresponding to 1000 mAh g^{-1} in the $LiPF_6$ organic electrolyte. The organic electrolyte was chosen because silicon nanowires showed higher initial charge capacities in the organic electrolyte compared to IL electrolyte. The initial discharge cycles were performed at C/20, and then increased to C/10, as shown in Fig. 6A. The battery showed the steady cycle life for more than 200 cycles without degradation at this higher discharge capacity and rating. Fig. 6B shows the voltage profile of

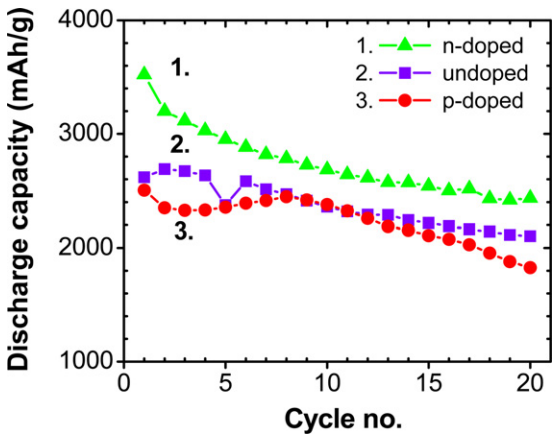

Fig. 7. Effect of doping (n and p type) on the capacity and cycle life of the Si nanowire anode in organic electrolyte. The performance of the nominally undoped nanowires is shown for comparison.

the charge–discharge cycles for the cell during the first 20 cycles and after 185 cycles. It was observed that the cell voltage gradually increased with additional cycles. For example, the cell voltage on the 20th cycle (1000 mAh g^{-1} capacity) was 0.45 V vs. Li^+/Li, which increased to 0.65 V after the 200th cycle. The reason for the increase in cell voltage could be due to limited degradation of the nanowire electrode, which lowers the overall electrode area and volume. Hence, a higher degree of delithiation is needed for the remaining active Si to provide for the original 1000 mAh g^{-1} discharge target capacity. From the values of cell potential measured at the end of 200th cycle, it appears that cell could have been cycled many more times, based on similar cycling studies.

Thus, limited-capacity cycling with voltage cut-off limits improved the battery cycling performance. It should be reemphasized that all of the cycling tests were accomplished with Si nanowires in the absence of binders or conductive agents. The use of binders and conductive agents, especially with IL electrolytes, offers a potential opportunity to further extend the battery life of Si nanowire electrodes.

A series of experiments were performed to explore the effect of doping on the capacity and cycle life of the nanowire anode. The SIMS measurement was done to estimate the concentration of B and P impurities in the nanowire mat. The details of the analytical procedure are given in the Supplementary information. Sample curvature and surface roughness of nanowires resulted in lower ion yield compared to flat sample probed at same beam current. To account for this lower yield, and the non-uniform sample coverage within the beam raster area during measurements, dopant signals were normalized with respect to the ^{30}Si intensity. By comparing the normalized dopant signal intensities (B/Si) to a known standard, the concentration of B in p-doped nanowires was estimated to be 2×10^{19} atoms cm^{-3}, which was close to the gas phase boron concentration of 5×10^{19} atoms cm^{-3} during nanowire growth. Some B contamination was seen in undoped nanowires in range of 5×10^{17}–1.4×10^{18} atoms cm^{-3}. The phosphorus concentration in n-doped Si nanowires was calculated to be 2×10^{20} atoms cm^{-3}.

All measurements with doped nanowires were performed in the organic electrolyte, 1 M $LiPF_6$/EC/DMC, and the results are summarized in Fig. 7. The results obtained with nominally undoped nanowires are also shown for comparison. The first cycle charge and discharge capacities of n, p and undoped nanowires were 3955, 3064, 2696 mAh g^{-1} and 3522, 2619, and 2505 mAh g^{-1}, respectively. The corresponding 1 st cycle coulombic efficiencies were 89.1%, 85.5% and 92.9% for n, p and undoped nanowires, respectively. The n-doped nanowire showed better performance than

the p-doped nanowires in terms of both discharge capacity values and the cycle life. Both types of doping should have higher initial electrical conductivity than the undoped nanowire, however, no direct conductivity measurements were made due to the difficulty of contacting individual nanowires. Although higher conductivity is desirable, the loss in capacity with p-doping indicates that other factors contribute to the capacity. There are several possible effects on the Si including a higher number of defects and a shift in the Fermi level of the Si with respect to the electrolyte potential. In particular, the Fermi level of n-doped Si is closer to the redox potential for lithiation/delithiation, which can affect the charge transfer resistance for the charging and discharging process. These results are consistent with the recent theoretical calculations of Peng [22] on the effect of various doping on the activation energy barrier for Li intercalation. They calculated a high energy barrier (0.88 eV) of lithium surface intercalation for undoped and boron doped Si that retards the fast lithium transport. However, this energy barrier was reduced when Si is doped with either phosphorus or aluminum. Although the results reported here seem to agree in general with prior theoretical and experimental results [22,23], careful investigation to the extent of dopant incorporation and other impurities during growth and type of precursor, is needed understand its effect on electrical and electrochemical properties.

4. Conclusion

The performance of Si nanowire electrodes was evaluated in IL and organic electrolyte. Half-cell testing with an IL electrolyte showed good performance with charge and discharge capacities of 2014 and 1836 mAh g^{-1}. However, the electrode showed capacity fade of 20–30% both in IL and organic electrolyte after 50 cycles. In order to extend the battery life, the electrodes were cycled using a limited-capacity discharge protocol that reduced the fraction of lithium intercalated/deintercalated from the lattice, and thus limited the extent of volumetric expansion/contraction. This approach yielded improvements in the battery life and greater than 600 cycles at 321 mAh g^{-1} in the IL electrolyte was demonstrated. At the higher discharge capacity, 1000 mAh g^{-1}, the battery life was also extended. Finally, the effect of different doping types on the battery capacity and cycle life was evaluated. It was found that phosphorus doping of the nanowires showed the highest capacity in comparison to boron or nominally undoped nanowires.

Acknowledgments

The authors would like to thank Dr. Klaus Franzreb at Arizona State University for their assistance with SIMS measurement. This work was funded by the Semiconductor Research Corporation through the Interconnect Focus Center, one of six Focus Center Research Programs.

Appendix A. Supplementary data

Supplementary data associated with this article can be found, in the online version, at doi:10.1016/j.jpowsour.2012.01.061.

References

[1] M. Green, E. Fielder, B. Scrosati, M. Wachtler, J.S. Moreno, Electrochem. Solid-State Lett. 6 (2003) A75.
[2] C.K. Chan, H. Peng, G. Liu, K. McIlwrath, X.F. Zhang, R.A. Huggins, Y. Cui, Nat. Nanotechnol. 3 (2008) 31.
[3] M.-H. Park, M.G. Kim, J. Joo, K. Kim, J. Kim, S. Ahn, Y. Cui, J. Cho, Nano Lett. 9 (2009) 3844.
[4] R. Krishnan, T.-M. Lu, N. Koratkar, Nano Lett. 11 (2010) 377.
[5] A. Magasinski, P. Dixon, B. Hertzberg, A. Kvit, J. Ayala, G. Yushin, Nat. Mater. 9 (2010) 353.
[6] S.-H. Ng, J. Wang, D. Wexler, K. Konstantinov, Z.-P. Guo, H.-K. Liu, Angew. Chem. Int. Ed. 45 (2006) 6896.
[7] L.-F. Cui, Y. Yang, C.-M. Hsu, Y. Cui, Nano Lett. 9 (2009) 3370.
[8] H. Kim, J. Cho, Nano Lett. 8 (2008) 3688.
[9] F.-F. Cao, J.-W. Deng, S. Xin, H.-X. Ji, O.G. Schmidt, L.-J. Wan, Y.-G. Guo, Adv. Mater. 23 (2011) 4415.
[10] M.-S. Park, S. Rajendran, Y.-M. Kang, K.-S. Han, Y.-S. Han, J.-Y. Lee, J. Power Sources 158 (2006) 650.
[11] G.X. Wang, L. Sun, D.H. Bradhurst, S. Zhong, S.X. Dou, H.K. Liu, J. Alloys Compd. 306 (2000) 249.
[12] W. Wang, P.N. Kumta, J. Power Sources 172 (2007) 650.
[13] J.K. Lee, K.B. Smith, C.M. Hayner, H.H. Kung, Chem. Commun. 46 (2010) 2025.
[14] Y. He, X. Yu, Y. Wang, H. Li, X. Huang, Adv. Mater. 23 (2011) 4938.
[15] T. Song, J. Xia, J.-H. Lee, D.H. Lee, M.-S. Kwon, J.-M. Choi, J. Wu, S.K. Doo, H. Chang, W.I. Park, D.S. Zang, H. Kim, Y. Huang, K.-C. Hwang, J.A. Rogers, U. Paik, Nano Lett. 10 (2010) 1710.
[16] B. Hertzberg, A. Alexeev, G. Yushin, J. Am. Chem. Soc. 132 (2010) 8548.
[17] W.-R. Liu, M.-H. Yang, H.-C. Wu, S.M. Chiao, N.-L. Wu, Electrochem. Solid-State Lett. 8 (2005) A100.
[18] V.A. Sethuraman, M.J. Chon, M. Shimshak, V. Srinivasan, P.R. Guduru, J. Power Sources 195 (2010) 5062.
[19] L.-F. Cui, R. Ruffo, C.K. Chan, H. Peng, Y. Cui, Nano Lett. 9 (2008) 491.
[20] V. Chakrapani, F. Rusli, M.A. Filler, P.A. Kohl, J. Phys. Chem. C 115 (2011) 22048.
[21] C.K. Chan, R. Ruffo, S.S. Hong, R.A. Huggins, Y. Cui, J. Power Sources 189 (2009) 34.
[22] B. Peng, J. Chem. Phys. 133 (2010) 034701.
[23] B.R. Long, M.K.Y. Chan, J.P. Greeley, A.A. Gewirth, J. Phys. Chem. C 115 (2011) 18916.